

Full Counting Statistics for Number of Electrons Dwelling in a Quantum Dot

Yasuhiro Utsumi^{1,2}

¹*Condensed Matter Theory Laboratory, RIKEN, Wako, Saitama 351-0198, Japan*

²*Institut für Theoretische Festkörperphysik, Universität Karlsruhe, 76128 Karlsruhe, Germany*

(Dated: March 20, 2019)

We theoretically study the statistical distribution of electron number inside a quantum dot weakly coupled to source and drain leads. We find an exponential tail in the number distribution when there is no dot-state close to lead chemical potentials. The joint distribution of number and current reveals a clear correlation between two quantities. The quantum fluctuations caused by increasing tunnel coupling change qualitatively the number distribution.

PACS numbers: 73.23.Hk,72.70.+m

In the last decade, the theory of the full counting statistics (FCS) [1] has been established to characterize the nonequilibrium current fluctuations in mesoscopic conductors [2]. This scheme provides the distribution P of the time-averaged current during the measurement time t_0 , $I \equiv q/t_0$, where $q = \int_{-t_0/2}^{t_0/2} dt I(t)/e$ is the number of transmitted electrons. From P , one can obtain not only the first and second cumulants of current distribution, i.e. average current and noise, but also any order cumulant. The FCS study has been much stimulated by the advance in experiments recently [3, 4, 5, 6].

In the last few years, the third cumulant of current distribution has been measured for tunnel junctions [3, 4]. For a system of two series-connected tunnel junctions, a quantum dot (QD), the current distribution itself was experimentally obtained recently [5, 6]. The QD is a small confined region where the energy levels are discrete. It weakly couples to source (R) and drain (L) leads, and the only one level ϵ_0 contributes to the transport when the temperature T and the source-drain bias voltage times the electron charge eV is smaller than the level spacing (we use $k_B = \hbar = 1$): If the dot-level is tuned to sit inbetween chemical potentials of L and R leads, $\mu_R < \epsilon_0 < \mu_L$ ($eV = \mu_L - \mu_R$), electrons tunnel one by one. The recent experiments [5, 6] adopted the real-time electron-counting technique using quantum point contact (QPC) charge detectors. Therefore the measured quantity is the time evolution of electron number inside the QD, $n(t)$, quantized and fluctuating between $n_0 - 1/2$ and $n_0 + 1/2$ (n_0 is a half-integer). Nevertheless for $T \ll eV$ and $\mu_R < \epsilon_0 < \mu_L$, where the thermal fluctuations are suppressed and electrons tunnel in one direction, Gustavsson *et al.* [5] obtained the current distribution utilizing a one-to-one correspondence between a transition event $n_0 \mp 1/2 \rightarrow n_0 \pm 1/2$ and an incoming/outgoing tunneling event.

For now, the experiments have been performed in the weak tunneling case, where the FCS theory of the Master equation approach by Bagrets and Nazarov [7] works perfectly. The case for increasing tunnel coupling is also interesting because the quantum coherence shows up. However, the large coupling will spoil the two well re-

solved number states and, consequently, the one-to-one correspondence between transition and tunneling events. In addition, the electron counting by QPC cannot determine the direction of tunneling. For the bidirectional counting, an elaborate device, a double QD asymmetrically coupled to one QPC, is required as demonstrated by Fujisawa *et al.* [6]. Therefore it is relevant to provide the FCS theory directly supporting the QPC experiments. In this paper, we will extend the FCS for the time-averaged electron number $s \equiv \tau/t_0$, where $\tau = \int_{-t_0/2}^{t_0/2} dt n(t)$ is the dwell-time of electrons inside the QD. We will calculate the cumulant generating function (CGF) of the joint distribution for s and I and analyze its basic features for several cases. It turns out that even within the Markov approximation, the number distribution posses qualitatively different features than the current distribution does.

Noninteracting QD. – We adopt the resonant-level model (RLM) for a noninteracting QD,

$$\hat{H} = \sum_{rk} \varepsilon_k \hat{a}_{rk}^\dagger \hat{a}_{rk} + \epsilon_0 \hat{d}^\dagger \hat{d} + \sum_{rk} (V_r \hat{d}^\dagger \hat{a}_{rk} + \text{H.c.}), \quad (1)$$

where \hat{a}_{rk} annihilates an electron with wave vector k in the left/right lead ($r=L/R$) while, \hat{d} annihilates an electron in the QD. The third term describes the tunnel coupling between the leads and the QD. The electrons in the lead r obey the Fermi distribution $f(\omega - \mu_r) = 1/(e^{(\omega - \mu_r)/T} + 1)$ and the coupling strength $\Gamma_r = 2\pi \sum_k |V_r|^2 \delta(\omega - \varepsilon_k)$ is energy independent.

We sketch the derivation of the CGF for the joint distribution of q and τ , $\mathcal{W}(\lambda, \xi) = \sum_{k,l} (i\lambda)^k (i\xi)^l \langle\langle \delta q^k \delta \tau^l \rangle\rangle / (k! l!)$, using the Schwinger-Keldysh approach [8, 9]. First, we introduce auxiliary source fields, $\varphi_r(t)$ and $h(t)$, the phase of the tunneling matrix element $V_r \rightarrow V_r e^{i\varphi_r(t)}$ and the fluctuation of the dot-level $\epsilon_0 \rightarrow \epsilon_0 + h(t)$. Note that here the time t is defined on the Keldysh contour C . Then the source fields on upper/lower Keldysh contour $\varphi_{r\pm}$ and h_\pm are fixed as the counting fields, $\varphi_{r\pm}(t) = \pm \lambda_r/2 + \mu_r t$ and $h_\pm(t) = \pm \xi/2$, during the measurement $(-t_0/2 < t < t_0/2)$ and $\varphi_{r\pm}(t) - \mu_r t = h_\pm(t) = 0$ otherwise. With the above condition, the Keldysh generating functional is identical

to the CGF, $\mathcal{W}(\lambda, \xi) = -i \ln \int D[a_{rk}^*, a_{rk}, d^*, d] e^{i \int_C dt \mathcal{L}(t)}$, where \mathcal{L} is the Lagrangian corresponding to the Hamiltonian (1). Here the tunnel coupling is switched on adiabatically. Although counting fields λ_L and λ_R appear at this stage, the final result contains only the difference $\lambda \equiv \lambda_L - \lambda_R$ from the charge conservation [10]. We checked that the first derivative in ξ gives τ with an offset; $\partial \mathcal{W} / \partial(i\xi)|_{\xi=0} = \int_{-t_0/2}^{t_0/2} dt \langle [d^\dagger(t), d(t)] \rangle / 2 = \tau - t_0/2$ where $d(t)$ is in the Heisenberg picture and the average is performed over the Hamiltonian (1) without the tunneling term. From now on, we will omit the offset.

Since the action is quadratic in the Grassmann variables, a_{rk}^* , a_{rk} , d^* and d , the path-integral along C can be performed with a proper boundary condition [8, 11]. For long measurement time $t_0 \gg 1/\Gamma$, we obtain

$$\mathcal{W} = \frac{t_0}{2\pi} \int d\omega \text{Tr} \ln \left[(\omega - \epsilon_0) \tau_1 + \frac{\xi}{2} \tau_0 - \tau_1 \tilde{\Sigma}^\lambda(\omega) \tau_1 \right],$$

where $\tilde{\Sigma}^\lambda = \sum_{r=L,R} \exp(i\lambda_r \tau_1/2) \tilde{\Sigma}_r \exp(-i\lambda_r \tau_1/2)$ is a 2×2 matrix in the Keldysh space, $[\tau_0]_{ij} = \delta_{ij}$ and $[\tau_1]_{ij} = 1 - \delta_{ij}$. The self-energy $\tilde{\Sigma}_r$ consists of retarded, advanced and Keldysh components as

$$\tilde{\Sigma}_r(\omega) = \begin{bmatrix} 0 & \Sigma_r^A \\ \Sigma_r^R & \Sigma_r^K \end{bmatrix} = -i \frac{\Gamma_r}{2} \begin{bmatrix} 0 & -1 \\ 1 & 2 \tanh(\omega/2T) \end{bmatrix}.$$

Further straightforward calculations yield

$$\begin{aligned} \mathcal{W} = & \frac{t_0}{2\pi} \int d\omega \ln \left\{ 1 - |G^R(\omega)|^2 \left(\frac{\xi^2}{4} - \frac{\xi}{2} \sum_{r=L,R} \Sigma_r^K(\omega) \right) \right. \\ & + \mathcal{T}(\omega) f(\omega - \mu_L) [1 - f(\omega - \mu_R)] (e^{i\lambda} - 1) \\ & \left. + \mathcal{T}(\omega) f(\omega - \mu_R) [1 - f(\omega - \mu_L)] (e^{-i\lambda} - 1) \right\}, \quad (2) \end{aligned}$$

where $G^R(\omega) = 1/[\omega - \epsilon_0 - \sum_{r=L,R} \Sigma_r^R(\omega)]$ and we subtracted a constant in order to fulfill the normalization condition $\mathcal{W}(0, 0) = 0$. The transmission probability,

$$\mathcal{T}(\omega) = 4 |G^R|^2 \text{Im} \Sigma_L^R \text{Im} \Sigma_R^R = \frac{\Gamma_L \Gamma_R}{(\omega - \epsilon_0)^2 + \Gamma^2/4}, \quad (3)$$

$(\Gamma = \Gamma_L + \Gamma_R)$ is Lorentzian. Equation (2) is the main result of this paper. Note that Levitov-Lesovik's formula [1] is recovered for $\xi = 0$.

The integration in frequency can be performed for $T \gg \Gamma$ following the procedure in Sec. IV of Ref. [7]:

$$\mathcal{W}(\lambda, \xi) \approx \mathcal{W}^{(1)}(\lambda, \xi) = t_0 \Gamma_\Sigma (\sqrt{D} - 1)/2, \quad (4)$$

$$\begin{aligned} D = & 1 + 4 [\Gamma_L^+ \Gamma_R^- (e^{i\lambda} - 1) + \Gamma_R^+ \Gamma_L^- (e^{-i\lambda} - 1)] / \Gamma_\Sigma^2 \\ & + [2i\xi(\Gamma^+ - \Gamma^-) - \xi^2] / \Gamma_\Sigma^2, \quad (\Gamma_\Sigma = \Gamma^+ + \Gamma^-), \quad (5) \end{aligned}$$

where $\Gamma^\pm = \sum_{r=L,R} \Gamma_r^\pm$ and $\Gamma_r^\pm = \Gamma_r / (e^{\pm(\epsilon_0 - \mu_r)/T} + 1)$ is the tunneling rate of an electron into/out of the QD through the junction r within Fermi's Golden rule. Note that the condition $T \gg \Gamma$ is that for the Markov approximation and that Eq. (4) is the first order expansion of

Eq. (2) in Γ assuming $\xi \propto \Gamma$. Actually, $\mathcal{W}^{(1)}(\lambda, 0)$ is equal to the CGF in the Master equation approach for FCS [7]. We further checked that the first and second cumulants, $\langle\langle \delta\tau \rangle\rangle / t_0 = (\Gamma^+ - \Gamma^-) / (2\Gamma_\Sigma)$ and $\langle\langle \delta\tau^2 \rangle\rangle / t_0 = 2\Gamma^+ \Gamma^- / \Gamma_\Sigma^3$, and the covariance $\langle\langle \delta q \delta\tau \rangle\rangle = -2\langle\langle \delta q \rangle\rangle \langle\langle \delta\tau \rangle\rangle / (\Gamma_\Sigma t_0)$ are reproduced by the Master equation approach for the noise developed by Korotkov [12].

Exponential tail in the number distribution.— In the limit of $t_0 \rightarrow \infty$, the electron number distribution is obtained by the inverse Fourier transform within the saddle point approximation:

$$P(s) = \frac{t_0}{2\pi} \int_{-\infty}^{\infty} d\xi e^{\mathcal{W}(0, \xi) - it_0 s \xi} \approx e^{\mathcal{W}(0, \xi^*) - it_0 s \xi^*}, \quad (6)$$

where ξ^* satisfies the equation $it_0 s = \partial_\xi \mathcal{W}(0, \xi^*)$. Solid lines in Fig. 1 (a) are the number distribution derived from Eq. (4) in equilibrium for symmetric coupling ($eV = 0$ and $\Gamma_L = \Gamma_R$). When the dot-level is at the lead chemical potentials, $\epsilon_0 = 0$ (line A), the distribution is well fitted by the Gaussian distribution around $s \approx 0$ (dotted line), $P(s) \approx \exp[-(s t_0 - \langle\langle \delta\tau \rangle\rangle)^2 / (2\langle\langle \delta\tau^2 \rangle\rangle)]$. Around $s = \pm 1/2$, it is suppressed strongly from the Gaussian form. Since our RLM possess the particle-hole symmetry, the distribution appears symmetric for negative and positive ϵ_0 (not shown).

The deviation from the Gaussian distribution grows rapidly as the dot-level leaves away from the chemical potential. The range where the Gaussian distribution is valid shrinks and the long exponential tail appears (lines B and C). Especially, for $\mp \epsilon_0 \gg T$, the exponential distribution appears for $|s| < 1/2$ (line C); $P(s) \approx \exp[t_0 \Gamma_\Sigma (\pm s - 1/2)]$. The exponent is the decay rate of the excited state, namely for $\mp \epsilon_0 \gg T$, the decay rate of the empty/occupied state. The exponential tail in the number distribution of the QD is in clear contrast with that of the chaotic cavity where the Gaussian fluctuation is dominant and the second cumulant is proportional to the temperature times the dwell-time squared [13].

In the limit of the occupied or empty QD, a more careful treatment on the branch cut of the CGF is required. The square root in Eq. (4) reads $\sqrt{D} \approx \sqrt{(\pm 1 + i\xi/\Gamma_\Sigma)^2}$ for $\mp \epsilon_0/T \rightarrow \infty$. Then the branch is chosen uniquely from the normalization condition. We obtain $\mathcal{W}^{(1)} = \pm i t_0 \xi/2$ and thus the delta distribution $P(s) = \delta(s \mp 1/2)$. It supports our intuition that without the thermal and quantum fluctuations, an electron (a hole) is localized in the QD.

Spin effect in an interacting QD.— Up to now, we omitted the spin degrees of freedom. The trivial extension of the Hamiltonian (1) is to introduce the spin index $\sigma = \uparrow, \downarrow$ for fermions as, $\hat{a}_{rk} \rightarrow \hat{a}_{rk\sigma}$ and $\hat{d} \rightarrow \hat{d}_\sigma$. The extension results in the CGF twice as large as Eq. (2) because of the spin degeneracy. A nontrivial spin effect appears when the on-site Coulomb interaction $\hat{H}_{\text{int}} = U \hat{d}_{\uparrow}^\dagger \hat{d}_{\uparrow} \hat{d}_{\downarrow}^\dagger \hat{d}_{\downarrow}$ is accounted for. For simplicity, we will consider in the limit

$U \rightarrow \infty$, where the double occupancy is forbidden and the QD states are limited to $|\uparrow\rangle$, $|\downarrow\rangle$ and $|0\rangle$. Furthermore, we will discuss the high temperature regime $T \gg \Gamma$, where is relevant for the experiments [5, 6] and the Master equation approach [7] works.

We extend the Master equation approach to calculate the joint distribution. The CGF is obtained by finding eigenvalues of the following matrix,

$$\hat{L}_{\lambda,\xi} = \begin{pmatrix} \Gamma^- - i\xi/2 & 0 & -\Gamma^+(\lambda) \\ 0 & \Gamma^- - i\xi/2 & -\Gamma^+(\lambda) \\ -\Gamma^-(\lambda) & -\Gamma^-(\lambda) & 2\Gamma^+ + i\xi/2 \end{pmatrix}, \quad (7)$$

where $\Gamma^\pm(\lambda) = \Gamma_L^\pm e^{\pm i\lambda_L} + \Gamma_R^\pm e^{\pm i\lambda_R}$. Unlike the counting field λ in the off-diagonal components, the counting field ξ appears in the diagonal components: $\mp i\xi/2$ for the occupied/empty state. We found a unique eigen value satisfying the normalization condition Λ_{\min} . The resulting CGF, $\mathcal{W} = -t_0\Lambda_{\min}$, becomes Eq. (4) with Γ_r^+ replaced with $2\Gamma_r^+$. We also checked that the extention of the Master equation approach reproduces Eq. (4) for the RLM.

The inset of Fig. 1 (a) shows the equilibrium number distribution. We observe the exponential tail both for $\epsilon_0 \gg T$ and for $-\epsilon_0 \gg T$ (lines E and C), but with different exponents by a factor 2: In the former case, the excited state is $|\uparrow\rangle$ or $|\downarrow\rangle$, and the decay rate is $\Gamma_\Sigma = \Gamma$. In the latter case, the decay rate of the excited state, i.e. the empty state $|0\rangle$, is the sum of the spin-up and down tunneling rates $\Gamma_\Sigma = 2\Gamma$.

Joint distribution.— We discuss the correlation between current and number fluctuations when the dot-level sits in the center of the two chemical potentials for the symmetric RLM ($\Gamma_L = \Gamma_R$, $\mu_L = -\mu_R$ and $\epsilon_0 = 0$). For $\Gamma \ll eV$, the first order expansion Eq. (4) is valid, and we have obtained the covariance $\langle\langle \delta q \delta \tau \rangle\rangle$ proportional to $\langle\langle \delta q \rangle\rangle$ and $\langle\langle \delta \tau \rangle\rangle$. It is 0 for the symmetric condition and does not provide so much information. Figure 1 (b) is the contour plot of the joint distribution $\ln P(I, s)$ calculated using Eq. (4) at $T = 0$. The inverse Fourier transformation of CGF is performed within the saddle point approximation, $\ln P(I, s) \approx \mathcal{W}^{(1)}(\lambda^*, \xi^*) - i t_0 I \lambda^* - i t_0 s \xi^*$ where λ^* and ξ^* are obtained from $i t_0 I = \partial_\lambda \mathcal{W}(\lambda^*, \xi^*)$ and $i t_0 s = \partial_\xi \mathcal{W}(\lambda^*, \xi^*)$. We observe a clear feature: For the current smaller than the average value, the distribution of s is almost uniform, while, for larger current, there is a peak around $s = 0$. The feature in the joint distribution is characteristic at low temperatures. At high temperatures, two quantities behave independently [Fig. 1 (c)].

Large quantum fluctuations: Single-electron transistor and RLM.— We turn our attention to the effect of the large tunnel coupling on FCS for a metallic island, i.e. the single-electron transistor (SET) [11, 14, 15]. For the metallic island the energy levels are continuous. However, the single-electron charging energy E_C can be larger than the temperature and the low-energy physics is dominated by two island states with charges differing by

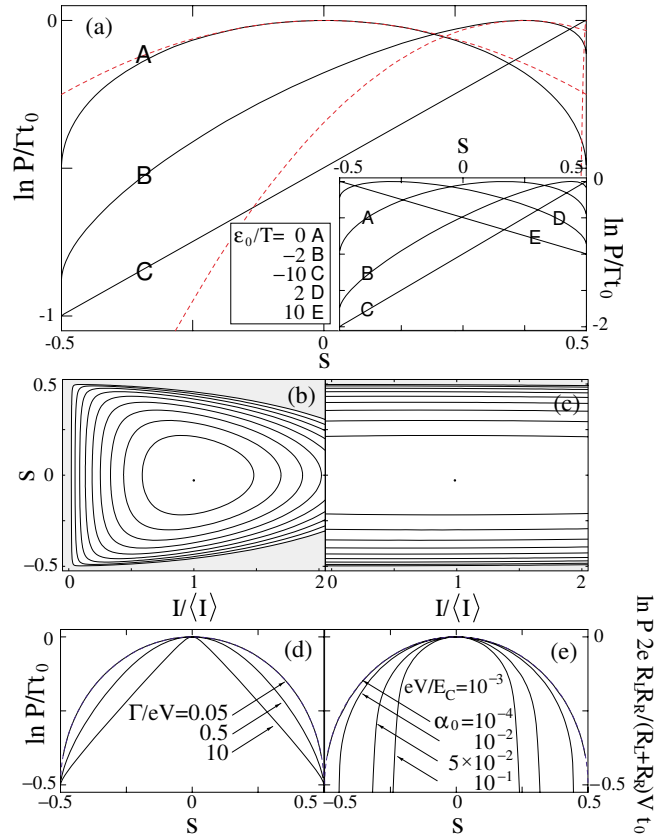


FIG. 1: The electron number distribution $P(s)$ of (a) noninteracting and interacting QD (inset) in equilibrium for symmetric case. Solid lines are for various dot-levels and dotted lines are for Gaussian distribution. Contour plot of the joint distribution $\ln P(q, \tau)$ for (b) $T/eV = 0$ and (c) 5 out of equilibrium. The function $\ln P(q, \tau)$ has a maximum value $\ln P(q, \tau) = 0$ at $I = \langle I \rangle$ and $s = 0$. The counter interval is $t_0\Gamma/20$ and $\ln P(q, \tau) \leq -t_0\Gamma/10$ for shedded region. The nonequilibrium number distributions of the resonant-level model (d) and the single-electron transistor (e) at $\epsilon_0 = \Delta_0 = 0$ and $T = 0$. Solid lines are for various Γ for (d) and α_0 for (e). The dotted lines (overlapping with solid lines) are obtained by the Master equation approach.

e. The energy difference between the two charge states Δ_0 is controlled by the gate voltage (Δ_0 corresponds to ϵ_0 for the RLM). The Hamiltonian is written with a pseud spin-1/2 operator $\hat{\sigma}$ acting on the two charge states as, $\hat{H} = \sum_{r=L,R,I} \sum_{kn} \epsilon_{rk} \hat{a}_{rkn}^\dagger \hat{a}_{rkn} + \Delta_0 \hat{\sigma}_z/2 + \sum_{r=L,R} \sum_{kk'n} (T_r \hat{a}_{Ik'n}^\dagger \hat{a}_{rk'n} \hat{\sigma}_+ + \text{H.c.})$, where \hat{a}_{rkn}^\dagger creates an electron with wave vector k in the left or right electrode or island ($r=L,R,I$). The tunneling process is assumed to preserve the channel (including spin) n . The junction conductance is related with the tunneling matrix element T_r , the number of channels N_{ch} and the electron DOS ρ_r as $1/R_r = 2\pi e^2 N_{\text{ch}} |T_r|^2 \rho_I \rho_r$. A measure for the tunneling strength is the dimensionless conductance $\alpha_0 = \alpha_0^L + \alpha_0^R$, where $\alpha_0^r = 1/2\pi e^2 R_r$ [14].

For the SET, the source fields, φ_r and h , are in-

troduced as $T_r \rightarrow T_r e^{i\varphi_r(t)}$ and $\Delta_0 \rightarrow \Delta_0 + h(t)$ [11]. They are fixed exactly in the same way as in the RLM case. In the following, we will apply the approximation developed in Refs. [11, 15] for large number of channels N_{ch} . The approximation is exact up to the second order in α_0 and it reproduces the renormalization of parameters consistent with the renormalization group analysis [16]. The extention to deal with an additional counting field ξ is straightforward. The result is formally the same as Eq. (2) but the Keldysh and retarded components of the self-energy are replaced with those of SET; $\Sigma_r^K(\omega) = -2i\pi\alpha_0^r(\omega - \mu_r)$ and $\Sigma_r^R(\omega) = 2\alpha_0^r[\text{Re}\psi(i(\omega - \mu_r)/2\pi T) - \psi(E_C/2\pi T) - \pi T/E_C] - i\pi\alpha_0^r(\omega - \mu_r)\coth[(\omega - \mu_r)/2T]$, where ψ is the digamma function. Consequently, the transmission probability Eq. (3) is replaced with

$$\mathcal{T}(\omega) = \frac{(2\pi)^2 \prod_{r=L,R} \alpha_0^r(\omega - \mu_r) \coth[(\omega - \mu_r)/2T]}{|\omega - \Delta_0 - \sum_{r=L,R} \Sigma_r^R(\omega)|^2}. \quad (8)$$

The effective transmission probability is the same as that in Ref. [14], which can describe the higher order inelastic cotunneling [17] current as well as the sequential tunneling current.

In the limit of $\alpha_0 \rightarrow 0$, the CGF in the Master equation approach is reproduced. The formal expression is the same as Eq. (4) with the tunneling rate of the RLM, Γ_r^\pm , replaced with that of the SET, $\Gamma_{rI/Ir} = \pm(\Delta_0 - \mu_r)/[(e^{\pm(\Delta_0 - \mu_r)/T} - 1)(e^2 R_r)]$. Therefore within the Markov approximation, though this time the tunneling rate is proportional to the bias voltage, the current and number obey qualitatively the same statistical distribution as that of the RLM.

However, it is not the case when the tunnel coupling increases and the quantum fluctuations are enhanced. We compare the saddle point solution of the nonequilibrium number distributions for the RLM [Fig. 1 (d)] and the SET [Fig. 1 (e)] at $\epsilon_0 = \Delta_0 = 0$ for the symmetric case ($\Gamma_L = \Gamma_R$, $\alpha_L^0 = \alpha_R^0$, and $\mu_L = -\mu_R$). When the tunneling is small, the number distributions for both cases approach the Master equation results [dotted lines overlapping with curves for $\Gamma/eV = 0.05$ (d) and for $\alpha_0 = 10^{-4}$ (e)]. For large tunnel coupling (Γ/eV and α_0), the fluctuations of electron number get stronger and thus the distributions for both cases shrink. However, a qualitative difference appears: For the SET, the width of the distribution shrinks, but for the RLM, the two sided exponential distribution like profile shows up. We can expect that it is related with the difference in the dominant higher order tunneling processes. For the RLM, the large tunnel coupling enhances the multiple tunneling process of a single electron, which preserves the phase coherence. For the SET with large N_{ch} , the coherent process, elastic cotunneling process, is suppressed as compared with the inelastic cotunneling process [14]. In the latter process, different electrons tunnel back and forth between

the leads and the metallic island. Therefore, the phase coherence is lost.

Before summarizing our findings, we note that the general expressions for the second cumulant and the covariance derived from our CGF (2),

$$\langle\langle \delta\tau^2 \rangle\rangle/t_0 = \Gamma^2 \int \frac{d\omega}{2\pi} \frac{f_{\text{eff}}(\omega)[1 - f_{\text{eff}}(\omega)]}{[(\omega - \epsilon_0)^2 + \Gamma^2/4]^2}, \quad (9)$$

$$\begin{aligned} \langle\langle \delta\tau\delta q \rangle\rangle/t_0 &= \Gamma \int \frac{d\omega}{2\pi} \frac{1/2 - f_{\text{eff}}(\omega)}{(\omega - \epsilon_0)^2 + \Gamma^2/4} \\ &\times \mathcal{T}(\omega)[f(\omega - \mu_L) - f(\omega - \mu_R)], \end{aligned} \quad (10)$$

where $f_{\text{eff}}(\omega) = \sum_r \Gamma_r f(\omega - \mu_r)/\Gamma$, are consistent with results obtained by the standard Keldysh diagrammatic approach [18] [Eqs. (87) and (88)], except for a factor and an offset.

In conclusion, we have extended the FCS theory for the statistical distribution of electron number in the QD and analyzed basic features for several cases. We found the exponential tail in the number distribution when the dot-level is far away from the lead chemical potentials and that the exponent depends on the spin degeneracy. We showed that the large tunnel coupling would narrow the number distribution generally: But for the symmetric noninteracting QD, where the multiple tunneling processes preserve the phase coherence, the two sided exponential distribution like profile appears. One measurable prediction for the presently available experimental setups is the joint distribution, which demonstrates that the number fluctuates differently if the current is larger or smaller than the average value.

I thank D. Bagrets, T. Fujisawa, A. Furusaki, Y. Gefen, T. Hayashi, T. Martin and G. Schön for valuable discussions. This work was supported by RIKEN Special PD Program and the DFG-Forschungszentrum “Centre for Functional Nanostructures”.

- [1] L. S. Levitov, H.-W. Lee, and G. B. Lesovik, *J. Math. Phys.* **37**, 4845 (1996).
- [2] *Quantum Noise in Mesoscopic Physics*, Vol. 97 of *NATO Science Series II: Mathematics, Physics and Chemistry* edited by Yu. V. Nazarov (Kluwer Academic Publishers, Dordrecht/Boston/London, 2003).
- [3] B. Reulet, J. Senzier, and D. E. Prober, *Phys. Rev. Lett.* **91**, 196601 (2003).
- [4] Yu. Bomze *et al.*, *Phys. Rev. Lett.* **95**, 176601 (2005).
- [5] S. Gustavsson *et al.*, *Phys. Rev. Lett.* **96**, 076605 (2006).
- [6] T. Fujisawa *et al.* (unpublished).
- [7] D. A. Bagrets, and Yu. V. Nazarov, *Phys. Rev. B* **67**, 085316 (2003).
- [8] A. Kamenev in *Strongly Correlated Fermions and Bosons in Low-Dimensional Disordered Systems*, edited by I. V. Lerner *et al.*, NATO Science Ser. II, Vol. 72 (Kluwer, Dordrecht, 2002).
- [9] K.-C. Chou *et al.*, *Phys. Rep.* **118**, 1 (1985); A. Kamenev in *Nanophysics: Coherence and Transport*, (Les Houches,

Volume Session LXXXI) eds. H. Bouchiat *et al.*, NATO ASI (Elsevier, Amsterdam, 2005).

[10] W. Belzig in *CFN Lecture Notes on Functional Nanostructures Vol. 1*, eds. K. Busch *et al.* Lecture Notes in Physics, Vol. 658 (Springer-Verlag, Berlin, 2004).

[11] Y. Utsumi *et al.*, Phys. Rev. B **67**, 035317 (2003).

[12] A. N. Korotkov, Phys. Rev. B **49**, 10381 (1994).

[13] S. Pilgram, and M. Büttiker, Phys. Rev. B **67**, 235308 (2003).

[14] H. Schoeller and G. Schön, Phys. Rev. B **50**, 18436 (1994).

[15] Y. Utsumi, D. S. Golubev, and G. Schön, Phys. Rev. Lett. **96**, 086803 (2006).

[16] K.A. Matveev, Sov. Phys. JETP. **72**, 892 (1991).

[17] D.V. Averin and Yu.V. Nazarov, Phys. Rev. Lett. **65**, 2446 (1990).

[18] S. Hershfield, Phys. Rev. B **46**, 7061 (1992).